

## The Resolution of the Volmer-Heyrovsky-Tafel Mechanism with a Normal Distribution of the Standard Gibbs Energy of Adsorption

M.R. Gennero de Chialvo and A.C. Chialvo\*

Programa de Electroquímica Aplicada e Ingeniería Electroquímica (PRELINE), Facultad de Ingeniería Química (UNL), Santiago del Estero 2829, 3000 Santa Fé, Argentina

Received: April 7, 1994; August 26, 1994

Tendo por base um modelo generalizado para a adsorção de hidrogênio recentemente proposto pelos autores, uma superfície heterogênea de eletrodo foi simulada através de uma função de distribuição normal da energia de Gibbs padrão de adsorção. Daí, o mecanismo de Volmer-Heyrovsky-Tafel para a reação de evolução de hidrogênio foi avaliado sob condição de estado estacionário sem qualquer aproximação cinética. Para cada rota, foi analisada a dependência da cobertura superficial e da densidade de corrente com o sobrepotencial. Conclui-se que a heterogeneidade superficial produz modificações substanciais no já conhecido comportamento cinético do mecanismo de Volmer-Heyrovsky-Tafel.

On the basis of a generalized model for hydrogen adsorption recently proposed by the authors, a heterogeneous electrode surface was simulated through a normal distribution function of the standard Gibbs energy of adsorption. The Volmer-Heyrovsky-Tafel mechanism for the hydrogen evolution reaction was then evaluated under steady state conditions without any kinetic approximation. The dependence of the surface coverage and the current density on the overpotential was analyzed for each route. It was concluded that surface heterogeneity produces substantial modifications in the previously known kinetic behavior of the Volmer-Heyrovsky-Tafel mechanism.

**Keywords:** adsorption process, hydrogen evolution

### Introduction

It is known that in the analysis of an electrode reaction process the behavior of an adsorbed intermediate can not be completely described through the Langmuir isotherm. This is due to the phenomena that govern the adsorption process, such as superficial and induced heterogeneity and lateral interactions, which produce a variation in the apparent standard Gibbs energy of adsorption  $\Delta G_{(a)}^{oapp}$  with the surface coverage  $\Theta^{1-4}$ , and which are also reflected in the reaction rate. The modeling of these microscopic phenomena is rather complex and particularly difficult in the case of superficial heterogeneity. An alternative treatment has recently been proposed<sup>5</sup> for simulation of hydrogen adsorption, consisting of the modeling of the electrode surface through a continuous succession of area elements, where a Langmuir type adsorption takes place. In this context, the standard Gibbs energy of the adsorbed hydrogen  $\mu_{H(a)}^o$  varies from one element of area to another, and this variation can be described through a distribution function.

The present work deals with the evaluation of the hydrogen evolution reaction (HER) on heterogeneous elec-

trode surfaces described through a normal distribution of the standard Gibbs energy of adsorption.

### Fundamental Aspects

#### Description of the distribution function

The differential element of area with a standard Gibbs energy of the adsorbed hydrogen ranging between  $\Delta\mu^o/RT$  and  $(\Delta\mu^o + d\Delta\mu^o)/RT$  can be written as<sup>5</sup>:

$$dA = f(\Delta\mu^o/RT) d(\Delta\mu^o/RT) \quad (1)$$

where  $f(\Delta\mu^o/RT)$  is the function that describes the variation of the standard Gibbs energy on the electrode surface. A normal distribution function has been adopted, which is given by the following expression:

$$f(x) = a e^{-\gamma x^2} \quad (2)$$

where:

$$x = \Delta\mu^o/RT = (\mu_{H(a)}^o - \mu_{H(a)}^{oM})/RT \quad (3)$$

$\mu_{H(a)}^{oM}$  is the standard Gibbs energy of the adsorbed hydrogen corresponding to the maximum value of the distribution function, and  $\gamma$  is a parameter. It should be noted that this parameter is related to the degree of heterogeneity  $r$  of the adsorption process,  $\mu_{H(a)}^{oM} \pm r$  being the standard Gibbs energy range within which one half of the total surface lies. The relationship between the parameter  $\gamma$  and the degree of heterogeneity  $r$  is then<sup>6</sup>:

$$\gamma = \frac{0.2274}{r^2} \quad (4)$$

The constant  $a$  of Eq. 2 was obtained by the integration of Eq. 1 over all the area  $A_o$ , varying  $x$  between a lower  $x_l$  and an upper  $x_u = |x_l|$  value:

$$a = \frac{A_o}{\int_{x_l}^{x_u} e^{-\gamma x^2} dx} \quad (5)$$

Furthermore, the fraction of surface  $A/A_o$  with a standard Gibbs energy of the adsorbed intermediate less than or equal to  $\mu_{H(a)}^o$  can be evaluated by inserting Eqs. 2 and 5 into Eq. 1 and integrating them:

$$\frac{A}{A_o} = \frac{\int_{x_l}^x e^{-\gamma x^2} dx}{\int_{x_l}^{x_u} e^{-\gamma x^2} dx} \quad (6)$$

#### Evaluation of the reaction rate

The macroscopic reaction rate  $u$  can be obtained through the integration of the microscopic reaction rate  $v$  over all of the electrode area, divided by  $A_o$ :

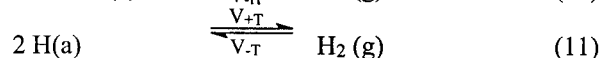
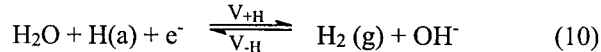
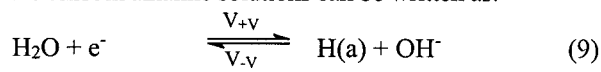
$$u = \frac{\int_{x_l}^{x_u} v(\eta, \Delta\mu^o) e^{-\gamma x^2} dx}{\int_{x_l}^{x_u} e^{-\gamma x^2} dx} \quad (7)$$

The corresponding expression for the macroscopic surface coverage  $\Theta$  as a function of the microscopic surface coverage  $\theta$  is:

$$\Theta = \frac{\int_{x_l}^{x_u} \theta(\eta, \Delta\mu^o) e^{-\gamma x^2} dx}{\int_{x_l}^{x_u} e^{-\gamma x^2} dx} \quad (8)$$

These generalized expressions allow the analysis of the effect of the heterogeneous adsorption on the reaction rate and surface coverage, respectively, including the equilibrium state.

Expressions for the reaction rate  $v(\eta, \Delta\mu^o)$  and for the surface coverage  $\theta(\eta, \Delta\mu^o)$  of each differential element of area are required for the resolution of Eqs. 7 and 8. The three elementary steps of the Volmer-Heyrovsky-Tafel mechanism for the HER in alkaline solutions can be written as:



The corresponding expressions for the reaction rate of each step were derived by applying the absolute reaction rate theory, taking into account that the variation of the standard Gibbs energy of the adsorbed hydrogen influences the reaction rate through the variation of the equilibrium reaction rate. These expressions were obtained from a given differential element of area and taking for reference the element of area with a Gibbs adsorption energy equal to  $\mu_{H(a)}^{oM}$ . The dependence of the resulting standard electrochemical Gibbs energy on the reaction coordinate can be treated like that of the electron transfer. In this case, a coefficient  $\beta_i$  of step  $i$  can be defined as a symmetry factor of the heterogeneous adsorption. The resulting expressions for the microscopic reaction rate of each step are the same as Eqs. 12-17 given elsewhere<sup>5</sup>, with a different reference element of area. Consequently, in this case  $v_{io}^e$  is the equilibrium reaction rate of step  $i$  corresponding to the differential element of area with a standard Gibbs energy of adsorption equal to  $\mu_{H(a)}^{oM}$ , and  $\theta_o^e$  is the equilibrium surface coverage of this reference element of area.

The resolution of the kinetic mechanism can be done through the Volmer-Heyrovsky (V-H) route, the Volmer-Tafel (V-T) route, or through both simultaneously (V-H-T). The steady state conditions are:

$$v = v_{+V} - v_{-V} = v_{+H} - v_{-H} \quad (12)$$

$$2v = v_{+V} - v_{-V} = 2(v_{+T} - v_{-T}) \quad (13)$$

$$2v = v_{+V} - v_{-V} + v_{+H} - v_{-H} =$$

$$2(v_{+H} - v_{-H} + v_{+T} - v_{-T}) \quad (14)$$

Introducing Eqs. 12-17<sup>5</sup> into Eqs. 12-14, the corresponding expressions of the microscopic reaction rate  $v(\eta, \Delta\mu^o)$  and the microscopic surface coverage  $\theta(\eta, \Delta\mu^o)$  can be obtained for each route. Then, by inserting them into Eqs. 7 and 8, the expressions for the macroscopic reaction rate and the macroscopic surface coverage are respectively obtained.

*The adsorption isotherm*

The dependence of the microscopic equilibrium surface coverage on hydrogen pressure can be obtained from the equilibrium reaction rate of the Tafel step<sup>5</sup>:

$$\Theta = \frac{K P_{H_2}^{1/2} e^{-x}}{1 + K P_{H_2}^{1/2} e^{-x}} \quad (15)$$

where  $P_{H_2}$  is the pressure of gaseous hydrogen and  $K = \exp(\Delta G_{(a)}^{oM}/RT)$ , and  $\Delta G_{(a)}^{oM} = \mu_{H(a)}^{oM} - g_{H_2}^*/2$  and  $g_{H_2}^*$  being the standard Gibbs energy of gaseous hydrogen. Inserting Eq. 15 into Eq. 8, the dependence of the macroscopic equilibrium surface coverage on hydrogen pressure is obtained:

$$\Theta^e = \frac{K P_{H_2}^{1/2} \int_{x_1}^{x_u} \frac{e^{-x} e^{-\gamma x^2}}{1 + K P_{H_2}^{1/2} e^{-x}} dx}{\int_{x_1}^{x_u} e^{-\gamma x^2}} \quad (16)$$

This equation gives the different types of adsorption isotherms that the proposed model can describe through the variation of the parameter  $\gamma$ , *i.e.* the intrinsic heterogeneity.

**Results**

*The characteristics of the distribution function used*

Figure 1a shows the shapes of the distribution function used in this work for different  $\gamma$  values. Limiting behaviors similar to those described in previous work<sup>5</sup> for the exponential distribution function can be observed. The possibility of generating different types of adsorption isotherms can be seen from Eq. 6 and Fig. 1b, where the variation of the relation  $A/A_0$  is plotted. It can be observed that when  $\gamma \leq 10^{-4}$  ( $\gamma \rightarrow 0$ ), the degree of heterogeneity is at a maximum and the following relation can be carried out:

$$\mu_{H(a)}^o = \mu_{H(a)}^{ol} + \Delta\mu^{om} (A/A_0) \quad (17)$$

where  $\Delta\mu^{om} = \mu_{H(a)}^{ou} - \mu_{H(a)}^{ol}$ . This equation corresponds to the basic description of the Temkin adsorption model<sup>7</sup>. However, when  $\gamma \geq 10^2$ , the degree of heterogeneity is null and therefore:

$$\mu_{H(a)}^o = \mu_{H(a)}^{oM} \quad (18)$$

This case can be clearly observed in Fig. 1, and corresponds to the Langmuirian adsorption.

*The dependence of  $\Delta G_{(a)}^{oapp}$  on  $\Theta^e$*

The dependence of  $\Delta G_{(a)}^{oapp}$  on  $\Theta^e$  can be written as:

$$\Delta G_{(a)}^{oapp} = \Delta G_{(a)}^{oM} + RTg(\Theta^e) \quad (19)$$

where the function  $g(\Theta^e)$  can be evaluated using the Frumkin isotherm:

$$\frac{\Theta^e}{1 - \Theta^e} e^{g(\Theta^e)} = K P_{H_2}^{1/2} \quad (20)$$

Therefore, from the theoretical dependence of  $\Theta^e$  on  $P_{H_2}$  established by the model, values of the function  $g(\Theta^e)$  can be calculated.

Figure 2 shows the relationships  $\Theta^e$  vs.  $K P_{H_2}^{1/2}$  (A) and  $g(\Theta^e)$  vs.  $\Theta^e$  (B) corresponding to the present model, for  $\Delta\mu^{om}/RT = 10$  and different values of the parameter  $\gamma$ . Taking into account that  $\Delta G_{(a)}^{oapp}$  is negative, a pseudo-linear

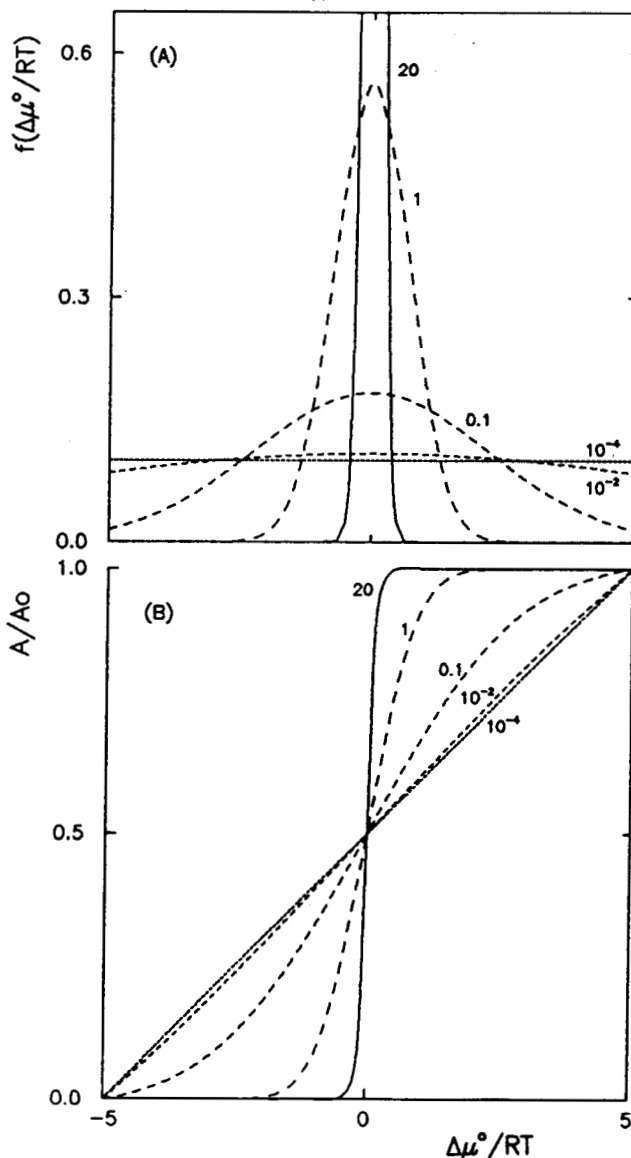


**Figure 1.** Influence of the parameter  $\gamma$  (values indicated in the figure) on the distribution function (A), and the relation  $A/A_0$  (B).

decrease in the apparent standard Gibbs energy of adsorption with the equilibrium surface coverage can be derived (Fig. 2b).

#### The dependence of $\ln(j/j_1^0)$ and on $\eta$

The dependence of the macroscopic reaction rate of the HER on the overpotential was evaluated for each reaction route: Volmer-Heyrovsky, Volmer-Tafel, and for both routes simultaneously. It was described in terms of current density, taking into account that  $j = 2Fu$  and  $j_1^0 = Fv_{1o}^e$ . Equation 7 was resolved by numerical analysis through computational calculation, following a procedure similar to that in previous work<sup>5</sup>. The dependence of the macroscopic surface coverage  $\Theta$  on  $\eta$  was also evaluated in each case using Eq. 8.

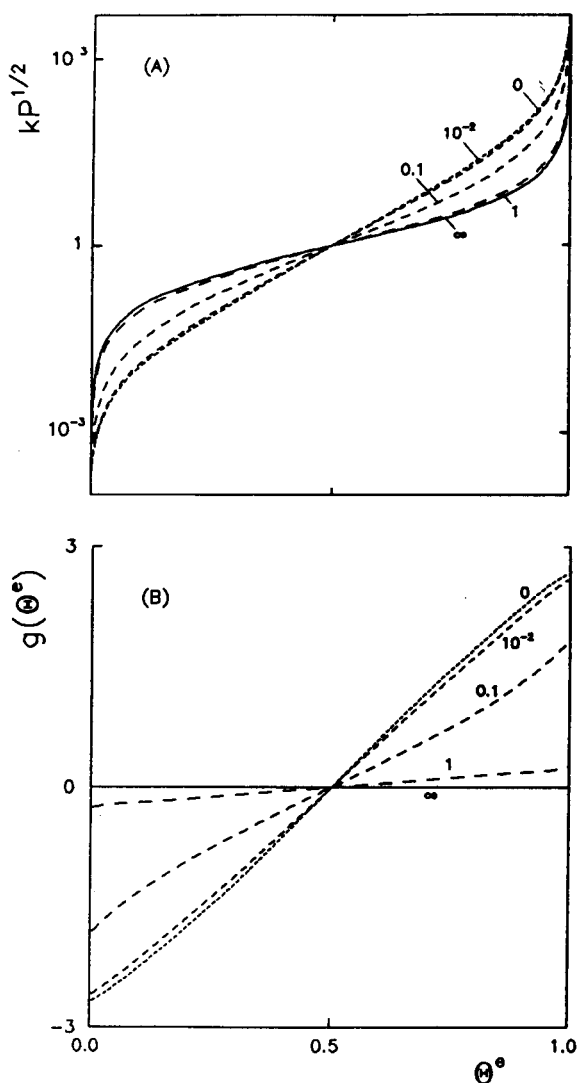


**Figure 2.** Dependence of the adsorption isotherm (A) and the function  $g(\Theta^e)$  (B) on  $\Theta^e$ , simulated with the proposed model for different  $\gamma$  values (indicated in the figure).

The relationships  $\Theta$  vs.  $\eta$  and  $\ln(j/j_1^0)$  vs.  $\eta$  for each route were calculated for different values of the model parameters. They vary between the following values:  $10^{-4} \leq \theta_o^e \leq 0.9999$ ,  $10^{-4} \leq m = j_2^0/j_1^0 \leq 10^6$  ( $i = 2,3$ ),  $0 \leq \gamma \leq \infty$  and  $-10 \leq \Delta\mu^0/RT \leq 10$  ( $10 \leq \Delta\mu^{om}/RT \leq 20$ ). In addition, T was set at 298.16 K and the symmetry factors  $\alpha_i$  and  $\beta_i$  were fixed for these calculations at 0.5.

#### The Volmer-Heyrovsky route

Figure 3 shows the  $\Theta$  vs.  $\eta$  and  $\ln(j/j_1^0)$  vs.  $\eta$  dependencies when  $\theta_o^e = 0.9999$ ,  $m_2 = 10^4$  and  $\Delta\mu^{om}/RT = 20$ , for different  $\gamma$  values. Two straight Tafel lines can be observed, with a marked dependence of the Tafel slope ( $3RT/2F \leq b \leq RT/F$ ) on  $\gamma$  in the low overpotential region.

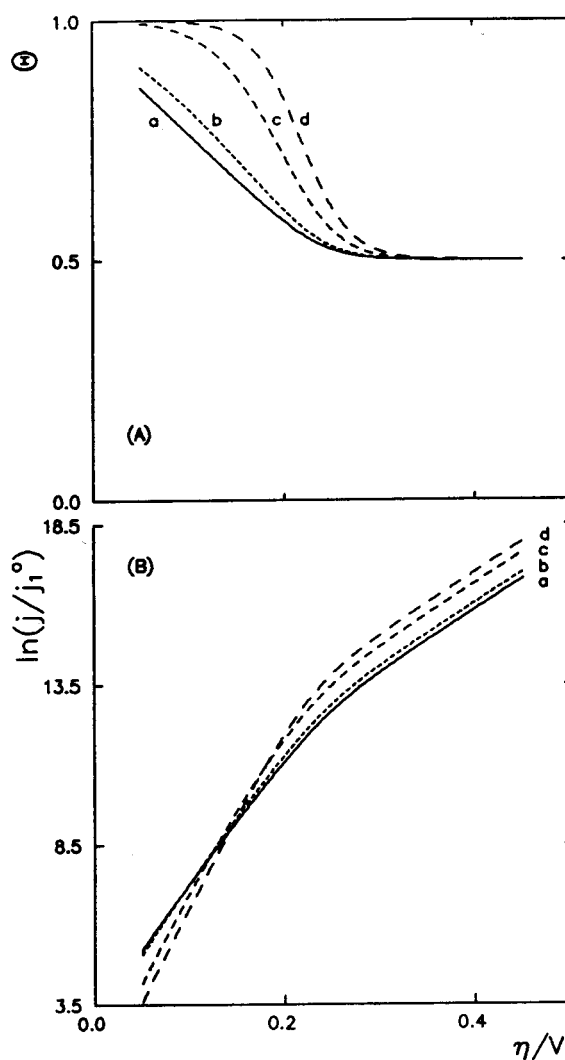


**Figure 3.** Dependence of  $\Theta$  (A) and  $\ln(j/j_1^0)$  (B) on  $\eta$  for the Volmer-Heyrovsky route.  $\theta_o^e = 0.9999$ ,  $m_2 = 10$  and  $\Delta\mu^{om}/RT = 20$ . a)  $\gamma = 0$ , b)  $\gamma = 10^{-2}$ , c)  $\gamma = 10^{-1}$ , and d)  $\gamma = \infty$ .

However, in the high overpotential region, the Tafel slope takes on a constant value equal to  $2RT/F$ .

The variation of the model parameters in the range stated above suggests that for this route the Tafel slope in the low overpotential region can vary in the following range:  $2RT/3F \leq b \leq 2RT/F$ . The Tafel slope in the high overpotential region was always equal to  $2RT/F$ . In addition, a unique Tafel line was found for  $m_2 = 1$  and independent of the  $\theta_0^e$  value, with  $b = 2RT/F$ .

#### The Volmer-Tafel route

As for the previous route, one case is illustrated in Fig. 4. It corresponds to  $\theta_0^e = 0.9$ ,  $m_3 = 10$  and  $\Delta\mu^{om}/RT = 15$ , for different  $\gamma$  values. In this case, the  $\ln(j/j_1^0)$  vs.  $\eta$  dependence shows a continuous curve. In contrast to the Volmer-

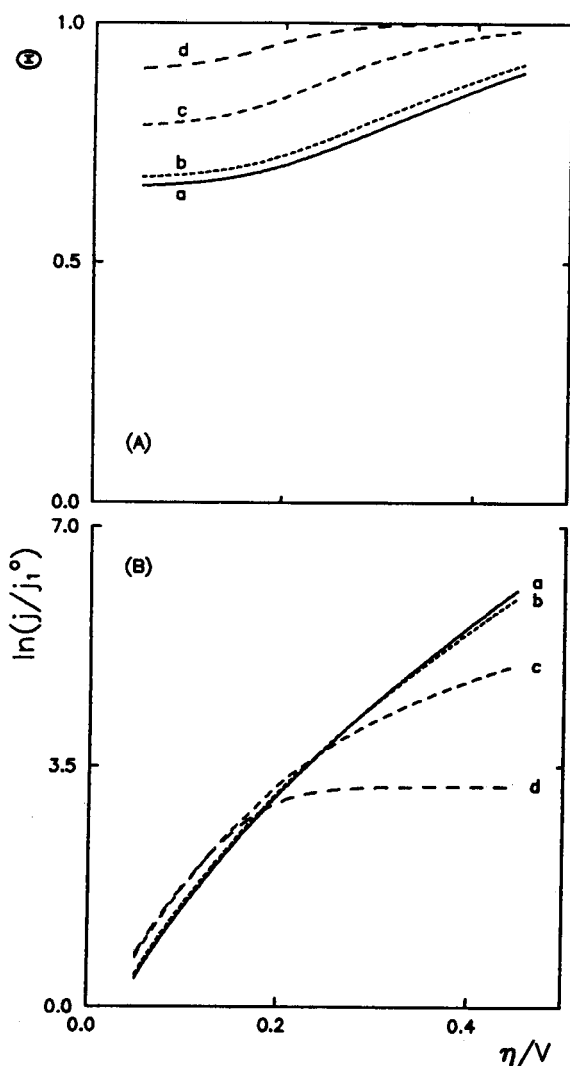


**Figure 4.** Dependence of  $\Theta$  (A) and  $\ln(j/j_1^0)$  (B) on  $\eta$  for the Volmer-Tafel route.  $\theta_0^e = 0.9$ ,  $m_3 = 10$  and  $\Delta\mu^{om}/RT = 15$ . a)  $\gamma = 0$ , b)  $\gamma = 10^{-2}$ , c)  $\gamma = 10^{-1}$ , and d)  $\gamma = \infty$ .

Heyrovsky route, the  $\gamma$  influence of the parameter is observed in the high overpotential region. The Tafel slope in the low overpotential region is near  $2RT/F$ , and in the high overpotential region it varies between the values:  $3RT/F \leq b \leq \infty$ .

The Tafel slope variation for the Volmer-Tafel route can be summarized as follows:  $RT/2F \leq b \leq 2RT/F$  for the low overpotential range, and  $2RT/F \leq b \leq \infty$  for the high overpotentials. A unique Tafel line has not been found for any values of the model parameters.

#### The Volmer-Heyrovsky-Tafel route

In this case, the large number of parameter combinations produces a large variety of  $\Theta$  vs.  $\eta$  and  $\ln(j/j_1^0)$  vs.  $\eta$  responses. In certain cases, these dependencies are improbable or unrealistic behaviors. Figure 5 illustrates an interesting case where a unique straight Tafel line is found for the whole range of overpotentials analyzed. The Tafel slope changes continuously from  $2RT/F$  for  $\gamma = \infty$  to  $3RT/F$  for  $\gamma = 0$ . Similar behavior has been shown by other authors for the HER in alkaline solutions<sup>8-12</sup>.

The  $\ln(j/j_1^0)$  vs.  $\eta$  dependence for the parallel course of the Volmer-Heyrovsky and Volmer-Tafel routes corresponds to the superposition of that dependence of each route. This combination greatly increases the descriptive capability with respect to the independent routes. It is worth noting the possibility of describing unique straight Tafel lines with different slope values. This is achieved by the application of both routes simultaneously, as well as by the distribution model used.

## Discussion and Conclusions

The present work theoretically determines the influence of the degree of heterogeneity on the HER described through the Volmer-Heyrovsky-Tafel mechanism and solved without kinetic approximations.

The contribution of the double layer was considered negligible, and the effects of anion adsorption as well as the changes of  $\alpha_i$  values with  $\eta$  were not taken into account. In addition, it was assumed that the adsorbed intermediate does not have superficial mobility, which means that the sites where water (or protons) is discharged through the Volmer step are the same as those where the desorption process takes place through the Heyrovsky and/or Tafel steps. These suppositions are in complete agreement with those made by other authors in recent studies of the HER on several metals<sup>13-17</sup>.

The results obtained show a marked influence of the degree of surface heterogeneity on kinetic behavior. This can be clearly seen in the comparison of curves (d) of Figs. 3-5 (homogeneous surface) with the other curves (heterogeneous surface). It should be noted that a Langmuirian

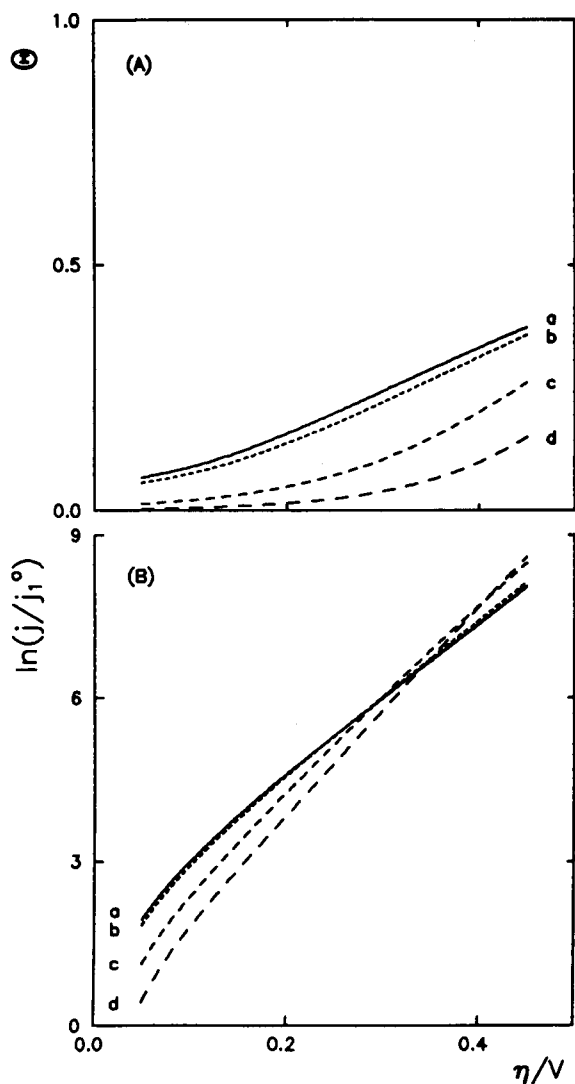


**Figure 5.** Dependence of  $\Theta$  (A) and  $\ln(j/j_1^0)$  (B) on  $\eta$  for the Volmer-Heyrovsky-Tafel route.  $\theta_0^e = 10^{-3}$ ,  $m_2 = 10^{-3}$ ,  $m_3 = 10^{-1}$  and  $\Delta\mu^{om}/RT = 15$ . a)  $\gamma = 0$ , b)  $\gamma = 10^{-2}$ , c)  $\gamma = 10^{-1}$ , and d)  $\gamma = \infty$ .

adsorption process can be applied when  $r < 0.05$ , and a Temkian one when  $r > 40$ .

Another aspect that deserves a brief analysis is the behavior of the Tafelian dependencies. The results show that the present model can describe a great variety of Tafel slopes (or the global transference coefficient  $\nu = RT/bF$ ), in spite of the symmetry factors of all steps being equal to 0.5. As such, the use of different  $\alpha_i$  values for one or more steps should extend the descriptive capability. Nevertheless, it should be taken into account that the symmetry factor directly ( $\alpha_i$ ) or indirectly ( $1 - \alpha_i$ ) reflects the reaction order of water (or  $H_3O^+$ ) in the expression of the reaction rate, and therefore experimental evidence<sup>18</sup> is essential for the selection of this value in order to obtain an adequate simulation.

It can be concluded that surface heterogeneity produces substantial modifications in the simulation of the kinetic behavior of the Volmer-Heyrovsky-Tafel mechanism and that erroneous interpretations of the experimental results can be induced if they are not taken into account.

#### Glossary

- $\mu_{H(a)}^0$ : standard Gibbs energy of the adsorbed hydrogen.
- $\gamma$ : parameter of the normal distribution function.
- $r$ : degree of heterogeneity.
- $\Theta$ : macroscopic surface coverage.
- $\theta$ : microscopic surface coverage.
- $u$ : macroscopic reaction rate.
- $v$ : microscopic reaction rate.
- $j$ : current density.
- $j_i^0$ : exchange current density of step  $i$ .
- $\eta$ : overpotential.

#### Acknowledgments

This work was supported by the Consejo Nacional de Investigaciones Científicas y Técnicas (CONICET, Argentina).

#### References

1. M. Boudart, *J. Amer. Chem. Soc.* **74**, 3556 (1952).
2. B.E. Conway and E. Gileady, *Trans. Faraday Soc.* **58**, 2493 (1962).
3. B.E. Conway, E. Gileady and M. Dzieciuch, *Electrochim. Acta* **8**, 143 (1963).
4. B.E. Conway and H. Angerstein-Kozłowska, *J. Electroanal. Chem.* **113**, 63 (1980).
5. M.R. Gennero de Chialvo and A.C. Chialvo, *J. Electroanal. Chem.* **209**, (1994).
6. S. Ross and J.P. Olivier, *On Physical Adsorption* (Interscience Publishers, USA, 1964), p.186.
7. T. Biegler and R. Woods, *J. Phys. Chem.* **73**, 3502 (1969).
8. B.V. Tilak, A.C. Ramamurthy and B.E. Conway, *Proc. Indian Acad. Sci. (Chem. Sci.)* **97**, 359 (1986).
9. G. Kreysa, B. Hakansson and P. Ekdunge, *Electrochim. Acta* **33**, 1351 (1988).
10. K. Lian, D.K. Kirk and S.J. Thorpe, *Electrochim. Acta* **36**, 537 (1991).
11. J.Y. Huot and L. Brossard, *J. Appl. Electrochem.* **18**, 815 (1988).
12. J.J. Podesta, R.C.V. Piatti, A.J. Arvia, P. Ekdunge, K. Juttner and G. Kreysa, *Int. J. Hydrogen Energy* **17**, 9 (1992).
13. E.R. Gonzalez, L.A. Avaca, G. Tremiliosi Filho, S.A. Machado and M. Ferreira, *Int. J. Hydrogen Energy* **19**, 17 (1994).
14. M. Okido, J.K. Depo and G.A. Capuano, *J. Electrochem. Soc.* **140**, 127 (1993).

15. P. Los and A. Lasia, *J. Electroanal. Chem.* **333**, 115 (1992).
16. Y. Choquette, L. Brossard, A. Lasia and H. Menard, *J. Electrochem. Soc.* **137**, 1723 (1990).
17. D.A. Harrington and B.E. Conway, *Electrochim. Acta* **32**, 1703 (1987).
18. D.R. Flinn and S. Schuldiner, *Electrochim. Acta* **19**, 421 (1974).